Electronic supplementary information (ESI) for the paper:

Efficient red luminescence from organic-soluble Au_{25} clusters by ligand structure modification

Ammu Mathew,[a] Elizabeth Varghese,[a] Susobhan Choudhury,[b] Samir Kumar Pal,[b] and T. Pradeep[a]*

[a] DST Unit of Nanoscience (DST UNS) and Thematic Unit of Excellence (TUE), Department of Chemistry, Indian Institute of Technology Madras, Chennai 600036, India.

[b] Department of Chemical Biological & Macromolecular Sciences, S. N. Bose National Centre for Basic Sciences, Block JD, Sector III, Salt Lake, Kolkata 700098, India

*E-mail: pradeep@iitm.ac.in

Table of contents

No.	Description	Pg no.
S1	Stability of UV-vis absorbtion spectral features of $Au_{25}SBB_{18}$ clusters	2
S2	Comparison of flourescence spectral chnges of cluster under various experimental conditions	3
S3	UV-vis absorption spectra of parent Au_{25} QCs and resultant red luminescent cluster	4
S4	NIR emission from parent $Au_{25}SBB_{18}$ QCs and red luminescent cluster	5
S5	Control experiments showing effect of BBSH thiol and Au(I)SBB thiolate with heating	6
S6	PL profile showing evolution of red luminescent cluster with time	7
S7	SEM and EDAX data from TLC plate of the red luminescent clusters	8
S8	ESI MS of $Au_{25}SBB_{18}$ and red luminescent cluster	9
S9	Comparison of TGA data from the QCs	10
S10	TEM images of $Au_{25}SBB_{18}$ and red luminescent Au_{29} clusters	11
S11	SEM and EDAX characterization of red luminescent Au_{29} cluster.	12
S12	Effect of addition of sodium borohydride to red luminescent Au_{29} cluster	13
S13	Picosecond life time decay of Au_{29} QCs upon excitation at different wavelengths.	14
S14	$Au_{25}SBB_{18}$-loaded silica gel experiment	15

Supporting information 1

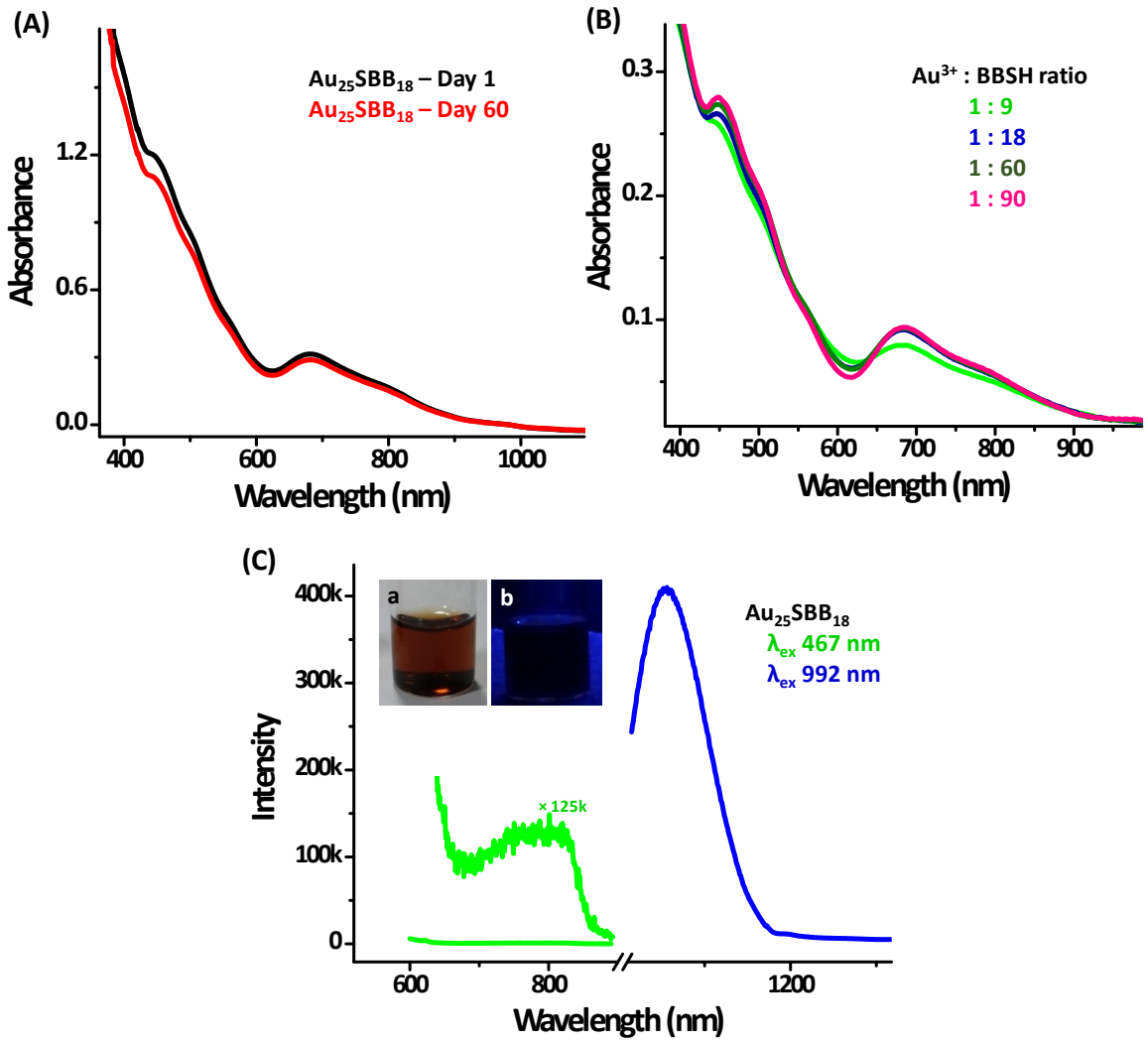

Figure S1. Stability of UV-vis absorbtion spectral features of $Au_{25}SBB_{18}$ clusters (A) with time and (B) against etching using excess BBSH thiol. Various Au:BBSH ratios used for etching are indicated. (C) Emission spectra of parent $Au_{25}SBB_{18}$ in the visible (λ_{ex} 467 nm, green trace) and NIR (λ_{ex} 992 nm, blue trace) regimes. An expanded version (125k times) of the original spectra is also shown for visualization. Inset shows photographs of the $Au_{25}SBB_{18}$ cluster under visible light (a) and UV light (b). Note that no observable visible luminescence is present from the solution.

Supporting information 2

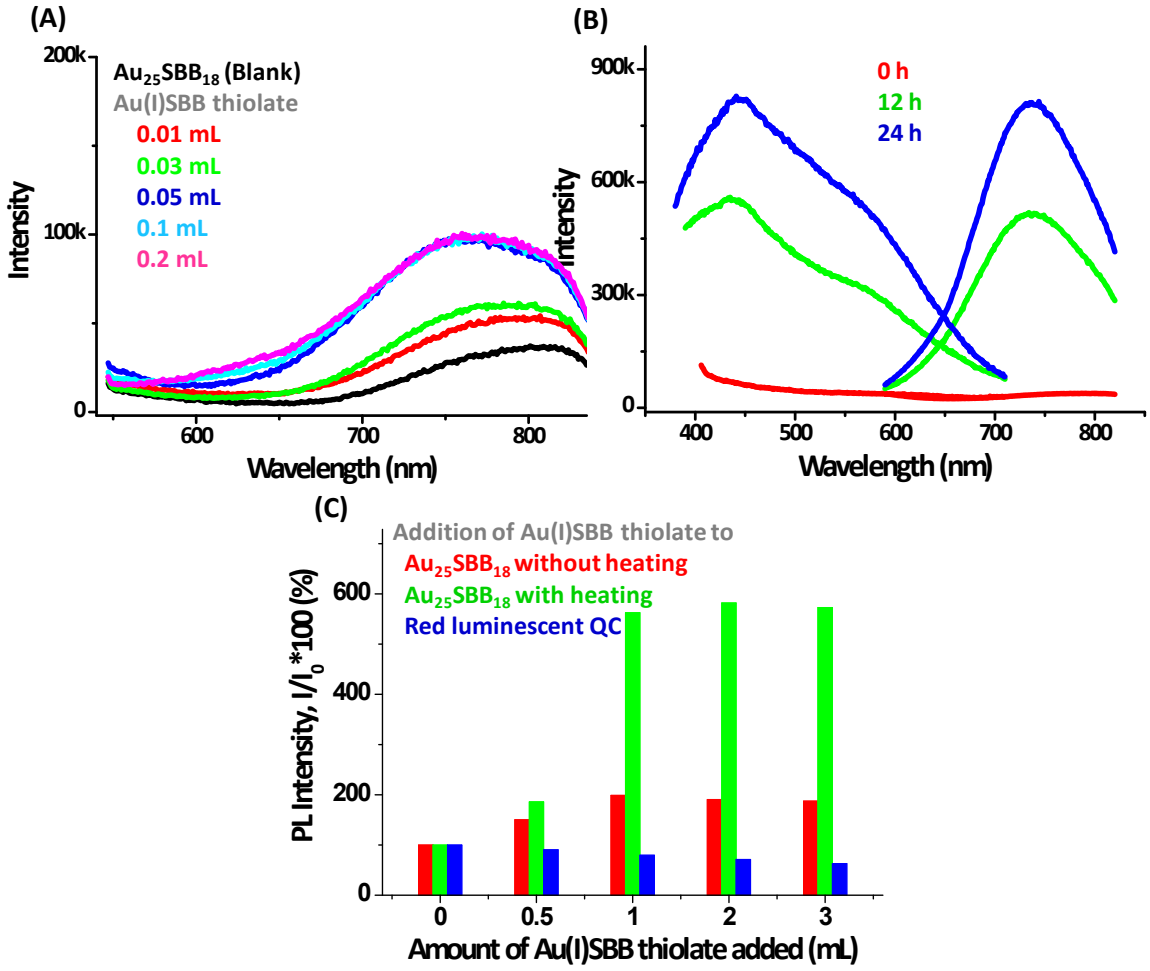

Figure S2. (A) Changes in the emission spectra (λ_{ex} 467 nm) of $Au_{25}SBB_{18}$ in the visible region upon addition of Au(I)SBB thiolate and heating for 2 h. (B) Evolution of excitation and emission spectra of the red luminescent cluster with increasing reaction time; 0 h (red trace), 12 h (green trace) and 24 h (blue trace). The time shown indicates the time for which sample was heated at 55 ^{o}C with stirring. The samples were cooled for 3 h before PL measurement. A 24 h thermal etching treatment was thus identified to obtain clusters with highest luminescence intensity. (C) Bar diagram comparing the changes in relative fluorescence intensity at 737 nm (ex 467 nm) upon addition of Au(I)SBB thiolate to pure Au_{25} followed by incubation for 24 h (red bars), pure Au_{25} with heating for 24 h (green bars) and to previously synthesized red luminescent clusters (blue bars).

Supporting information 3

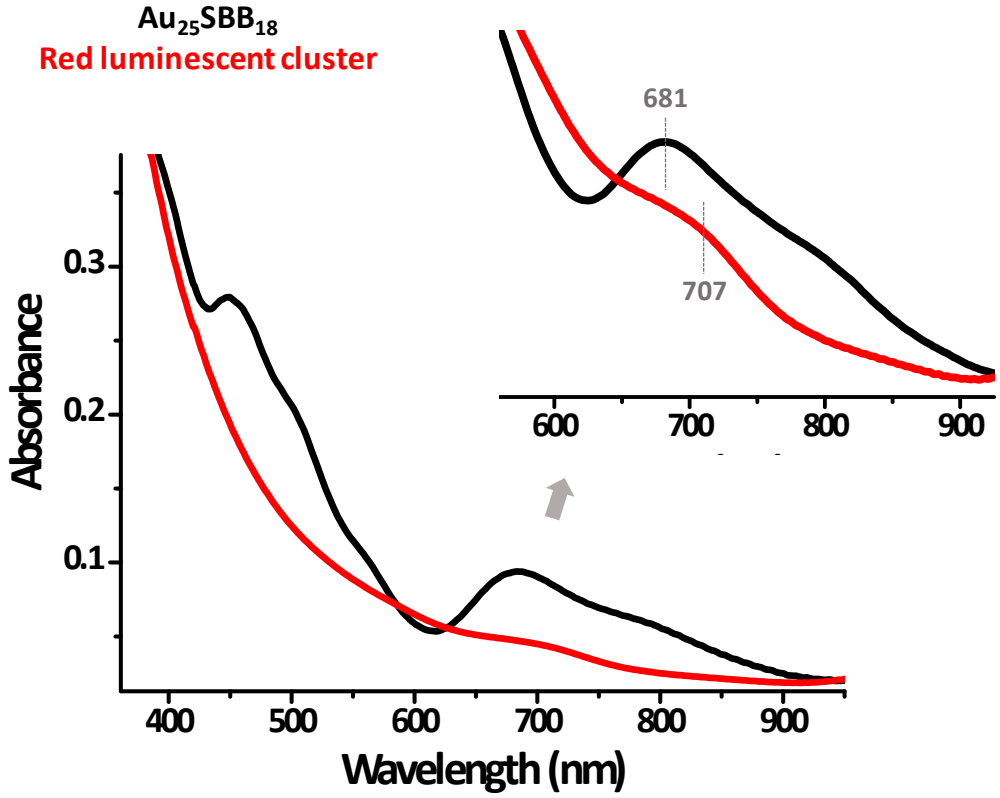

Figure S3. Comparison of UV-vis absorption spectra of parent $Au_{25}SBB_{18}$ (black trace) and resultant red luminescent cluster (red trace). Inset shows an expanded view of the spectra.

Supporting information 4

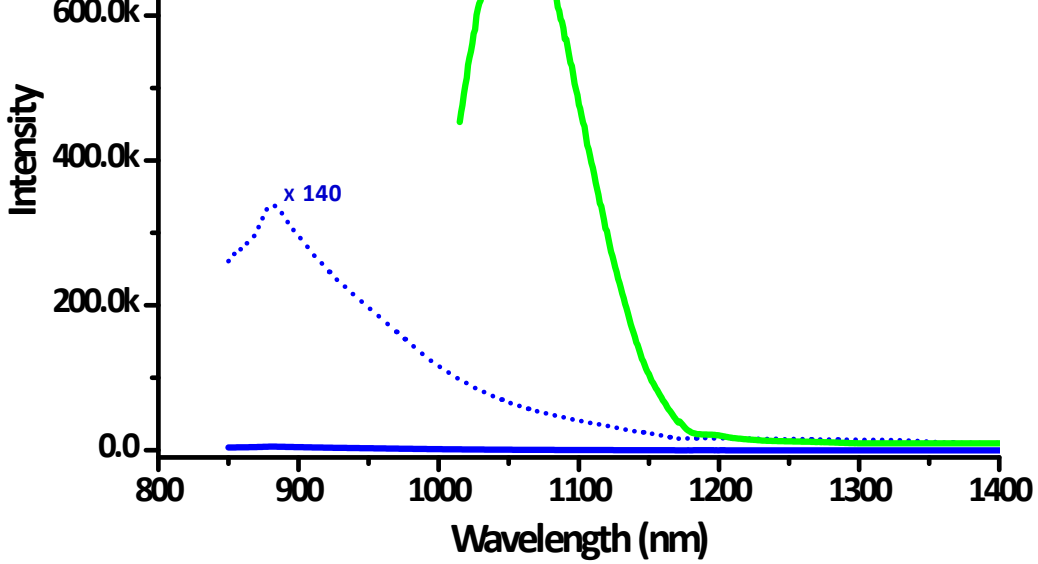

Figure S4. Comparison of emission in the NIR regime (excited at 992 nm) for parent $Au_{25}SBB_{18}$ QCs (green trace) and red luminescent Au_{29} (nucearity explained later) clusters (blue trace). An expanded spectra (140 times) showing the NIR features of the red luminescent clusters (blue dotted line) clearly indicates the absence of the prominent emission feature at 1030 nm (seen in parent Au_{25}) in the red luminescent cluster. Spectral features shows a blue shift accompaned by a drastic quenching after the reaction. Identical concentrations of both clusters are compared n the spectra under similar instrumental conditions.

Supporting information 5

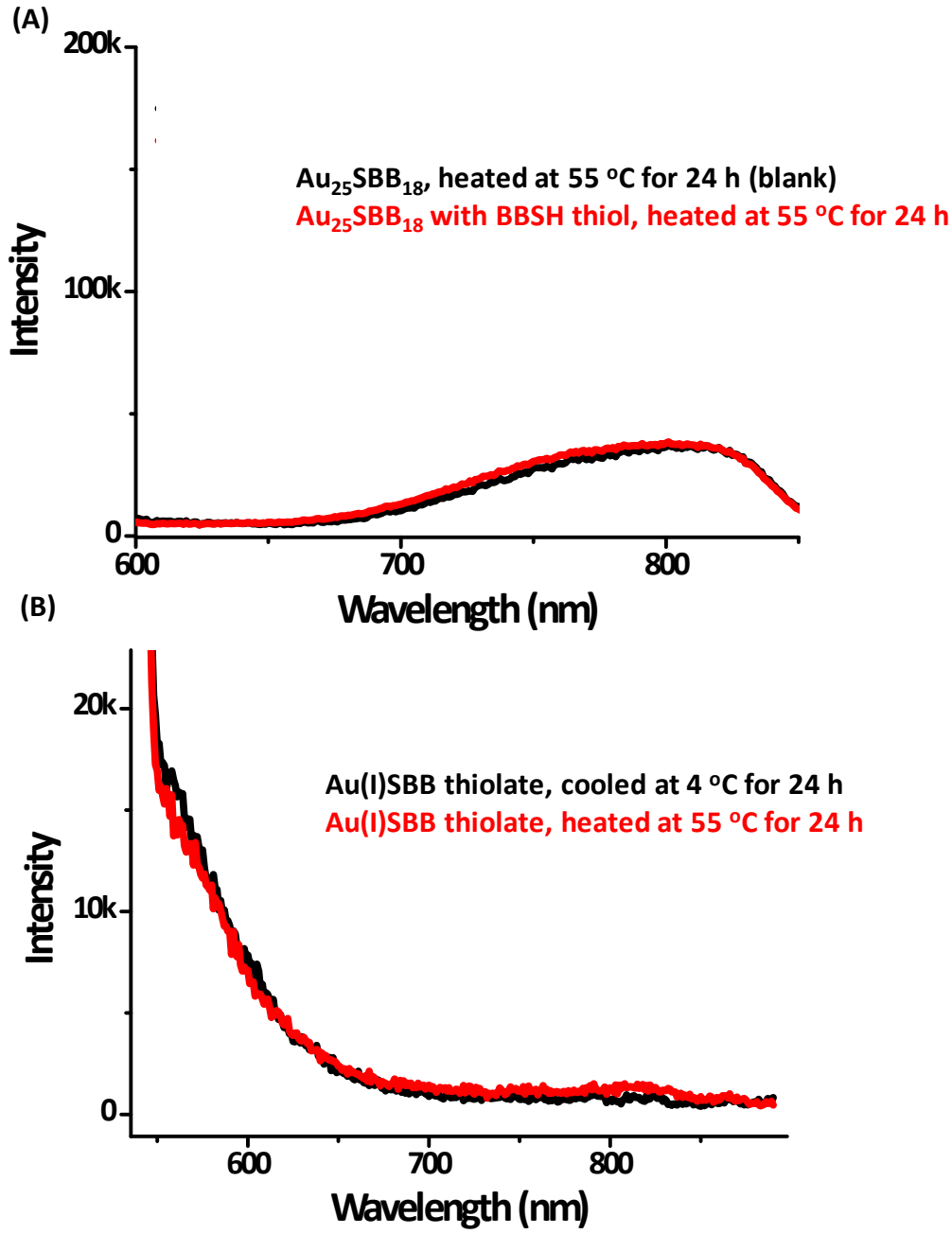

Figure S5. Control experiments showing the effect of emission spectra (ex 467 nm) of $Au_{25}SBB_{18}$ upon heating at 55 °C for 24 h in presence of similar concentrations of BBSH thiol (instead of Au(I)SBB thiolate used to synthesize red luminescent clusters) in comparison with parent clusters under identical conditions (A). (B) Effect of emission spectra of Au(I)SBB thiolate upon heating for 24 h at 55 °C. This validates that the visual luminescence enhancement observed upon heating Au_{25} QCs in presence of Au(I)SBB thiolate is neither a consequence of heating Au_{25} in presence of BBSH thiol nor an effect of heating Au(I)SBB thiolate for 24 h.

Supporting information 6

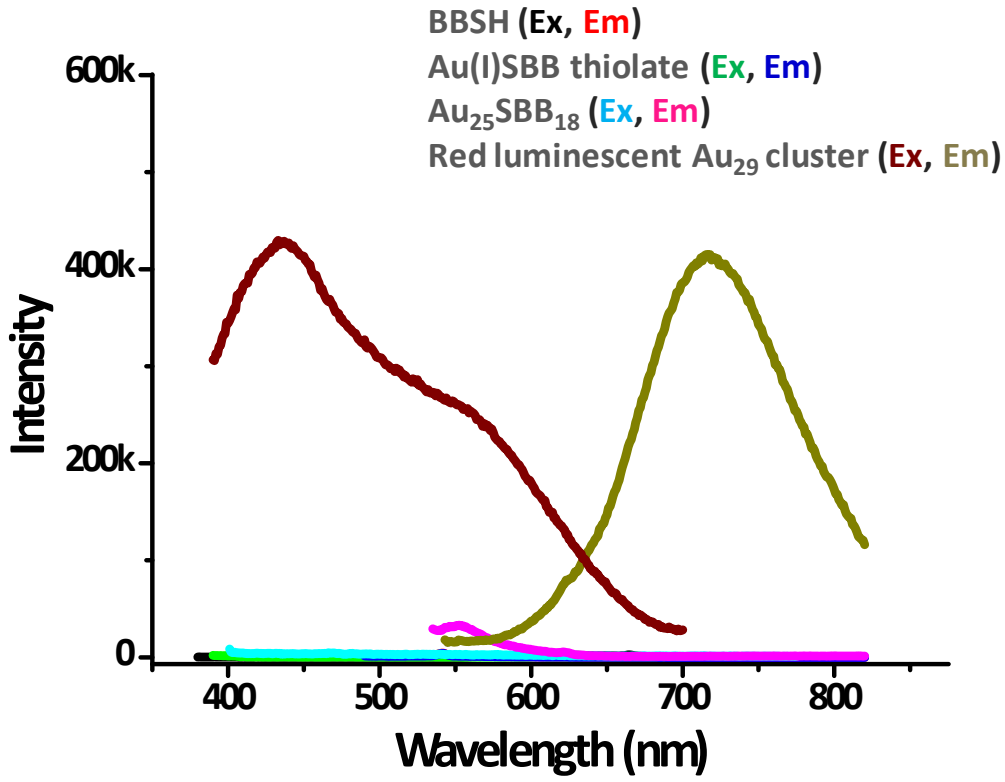

Figure S6. Comparison of excitation and emission spectra of the various reaction intermediates such as BBSH thiol (black and red trace), Au(I)SBB thiolate (green and blue trace), $Au_{25}SBB_{18}$ (cyan and pink trace) and red luminescent cluster (dark brown and tan trace) respectively. Solutions were diluted in THF so as to maintain identical concentrations (with respect to BBSH thiol). All solutions were measured at λ_{ex} 467 nm and λ_{em} of 737 nm. Slit width was kept at 3 nm for all measurements.

Supporting information 7

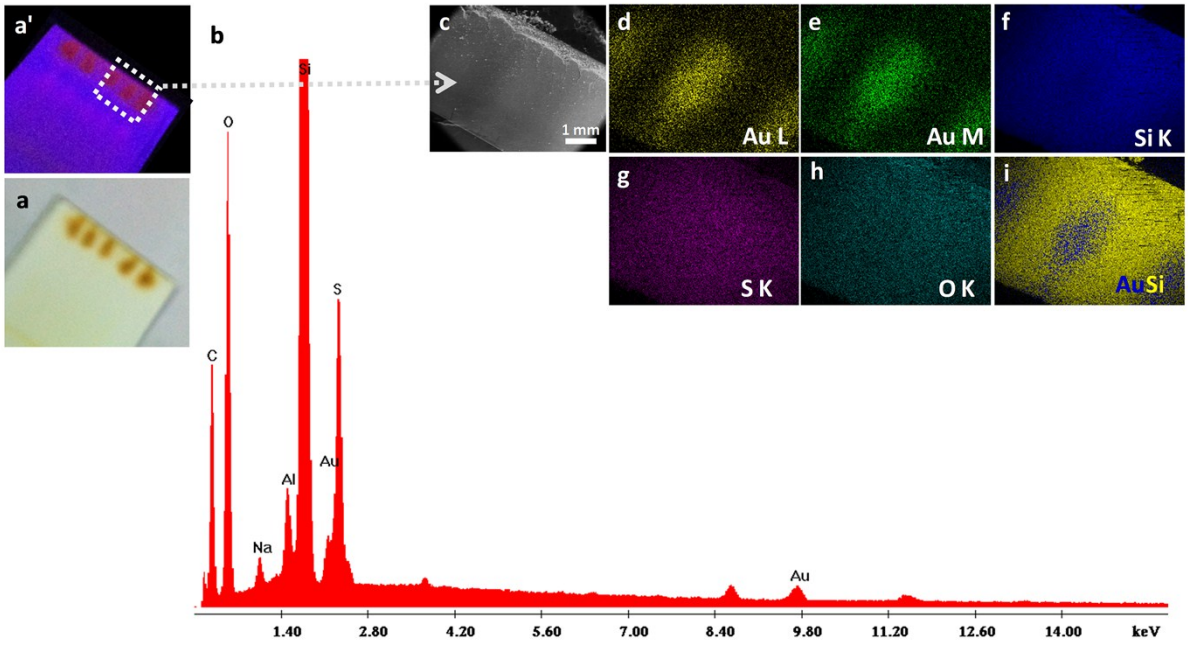

Figure S7. SEM (c), EDAX images (d-i) and EDAX spectrum (b) from the TLC plate with the separated red luminescent fraction (photograph shown as inset) under UV light (a′) and visible light (a).

Supporting information 8

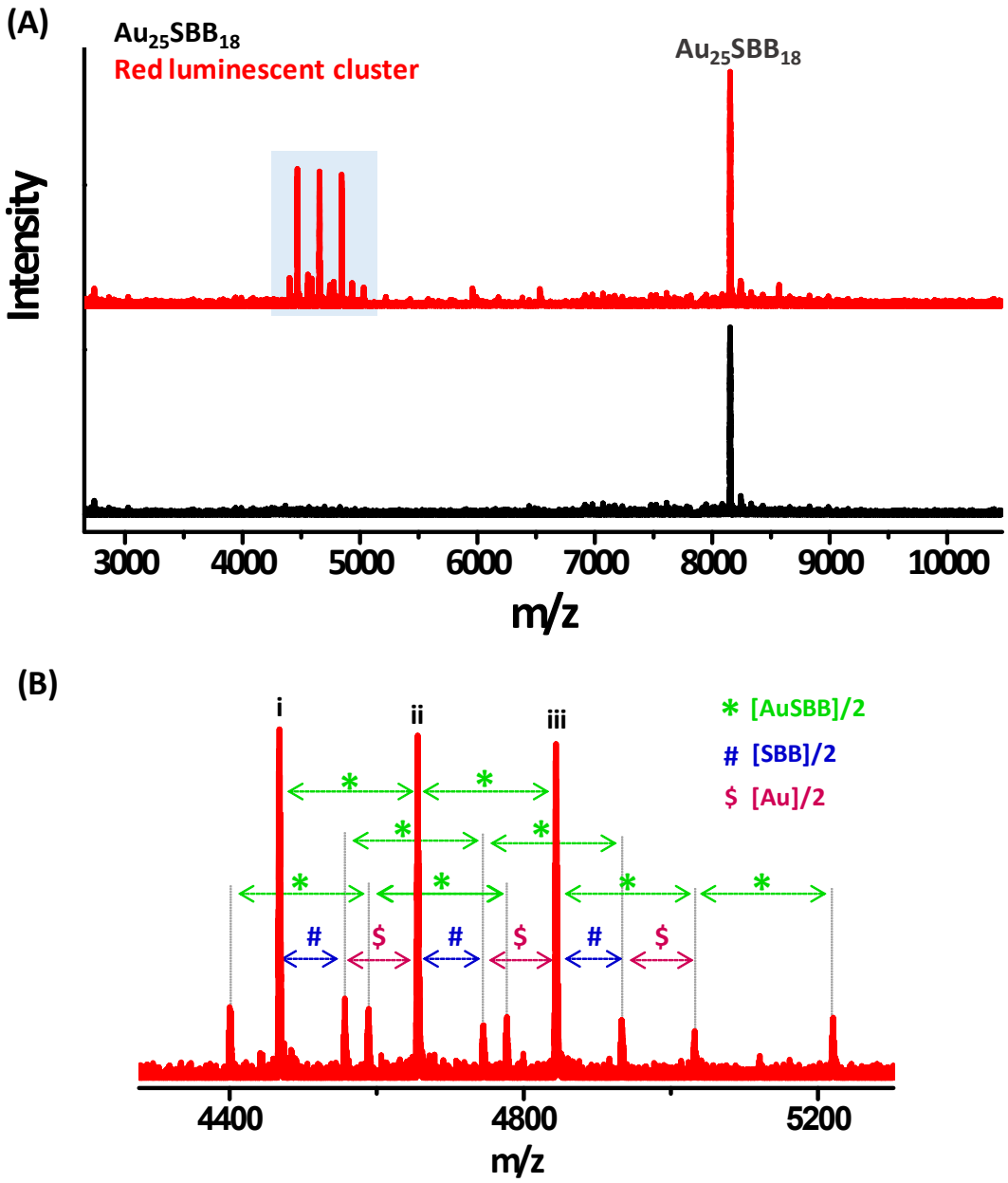

Figure S8. ESI MS of $Au_{25}SBB_{18}$ (black trace) and red luminescent cluster (red trace) in negative ion mode (A). Peak corresponding to Au_{25} is marked in the figure. (B) shows an expanded view of the area marked in (A). A difference of m/z 188, corresponding to (Au+SBB)/2, was observed between the three peaks marked i, ii and iii in the figure. Similar intensities of the peaks indicate fragmentation.

Supporting information 9

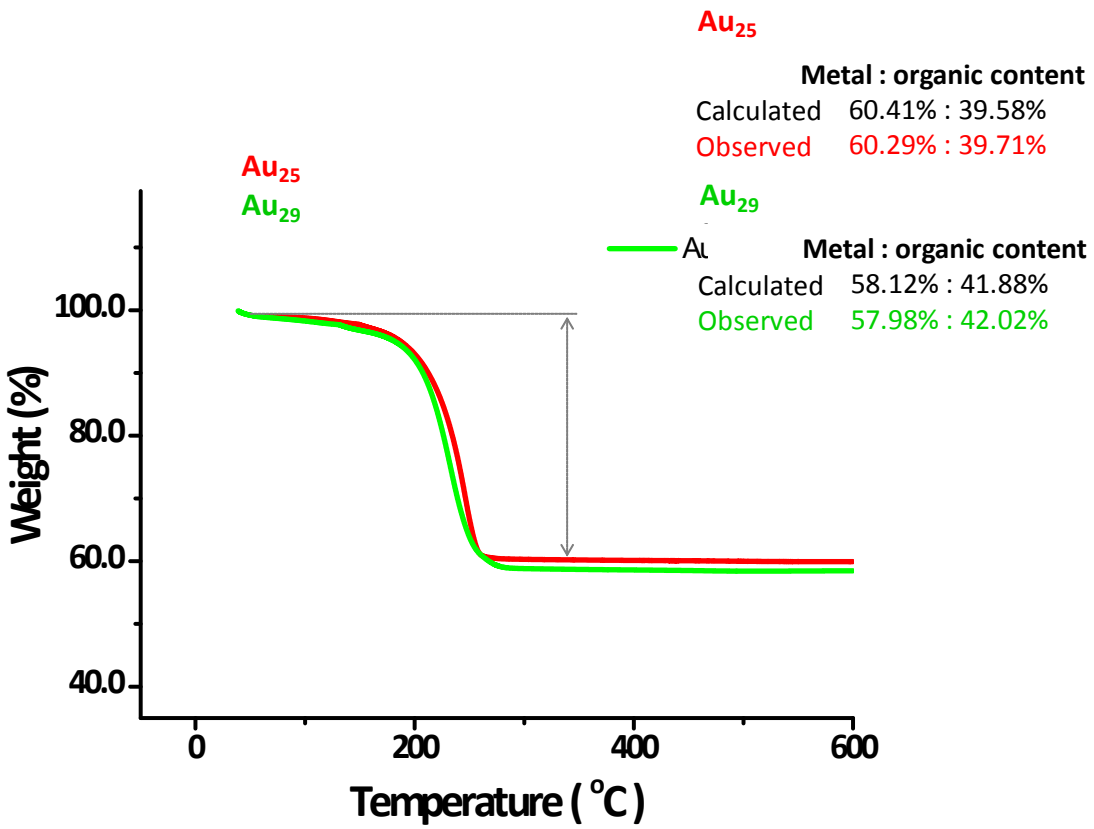

Figure S9. Comparison of TGA data from parent $Au_{25}SBB_{18}$ (red trace) and red luminescent Au_{29} QCs (green trace). Though both clusters show similar trend in thiolate desorption the organic content is more in the luminescent Au_{29} QC as shown. 2.51 mg of $Au_{25}SBB_{18}$ and 3.32 mg of Au_{29} was used for analysis under a N_2 atmosphere. Both experimental and calculated values (shown in the inset) are matching confirming the assignment.

Supporting information 10

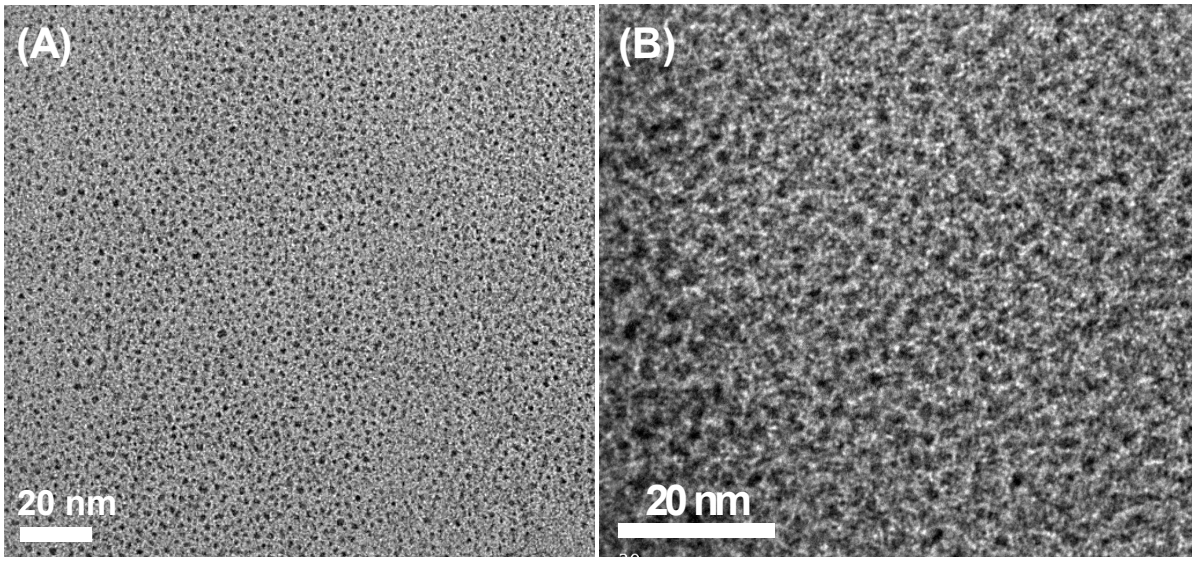

Figure S10. TEM images of (A) $Au_{25}SBB_{18}$ and (B) red luminescent Au_{29} clusters.

Supporting information 11

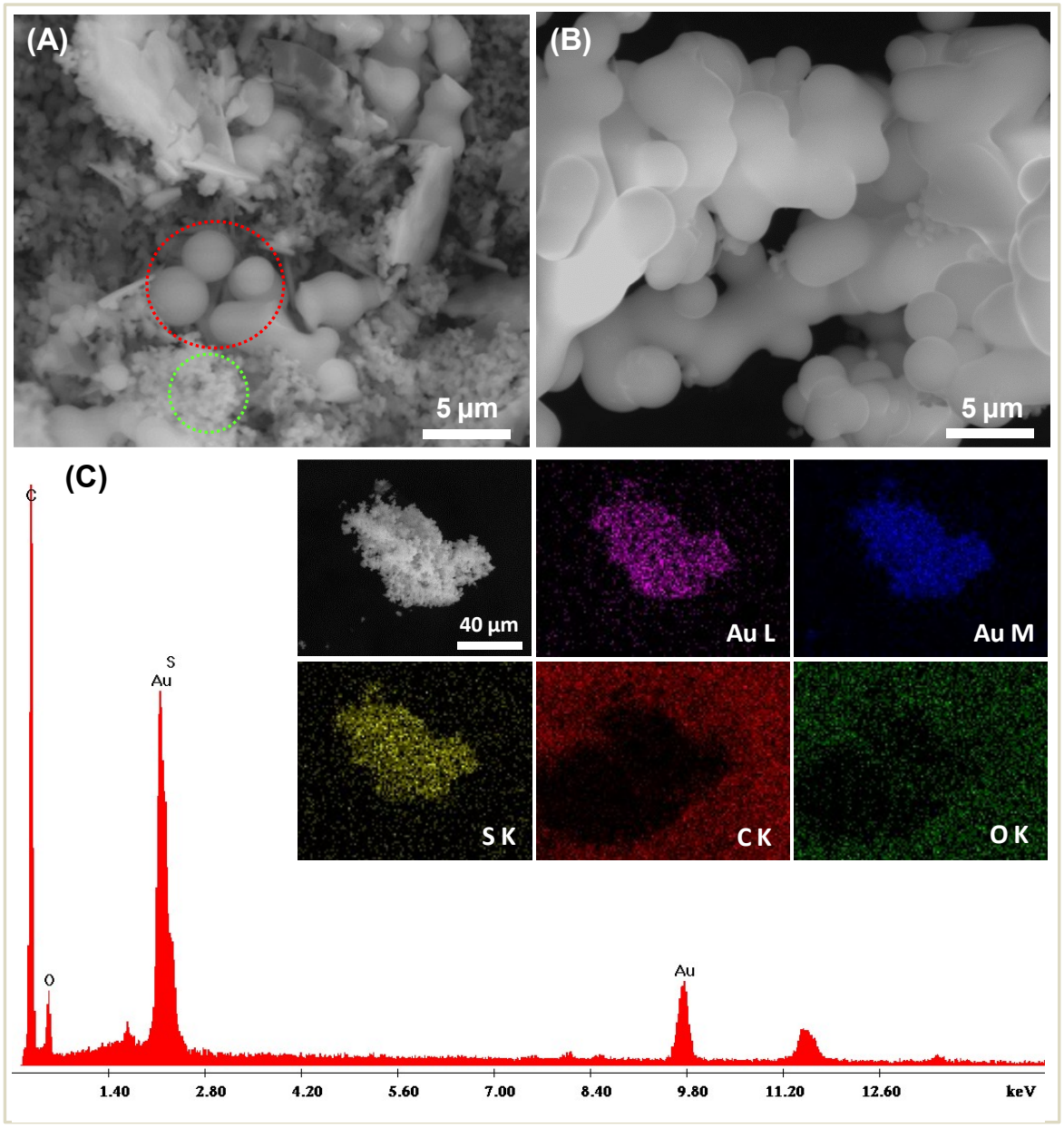

Figure S11. SEM (A, B) and EDAX (C) characterization of red luminescent Au@SBB cluster. SEM images at 6 h (A) and 24 h (B) of reacton are shown. A shows the crude cluster containing mixture of $Au_{25}SBB_{18}$ (indicated by green circle) and red luminescent Au_{29} cluster (red circle) obtained after 6 h of heating. Pure red luminescent $Au_{29}SBB_{23}$ cluster obtained after 24 h heating is shown in B. EDAX mapping and spectra are shown in (C). Carbon and aluminium are from the substrate used for the measurement. Contrast of carbon is low due to the use of carbon tape as the substrate. The scale is same for all images.

Supporting information 12

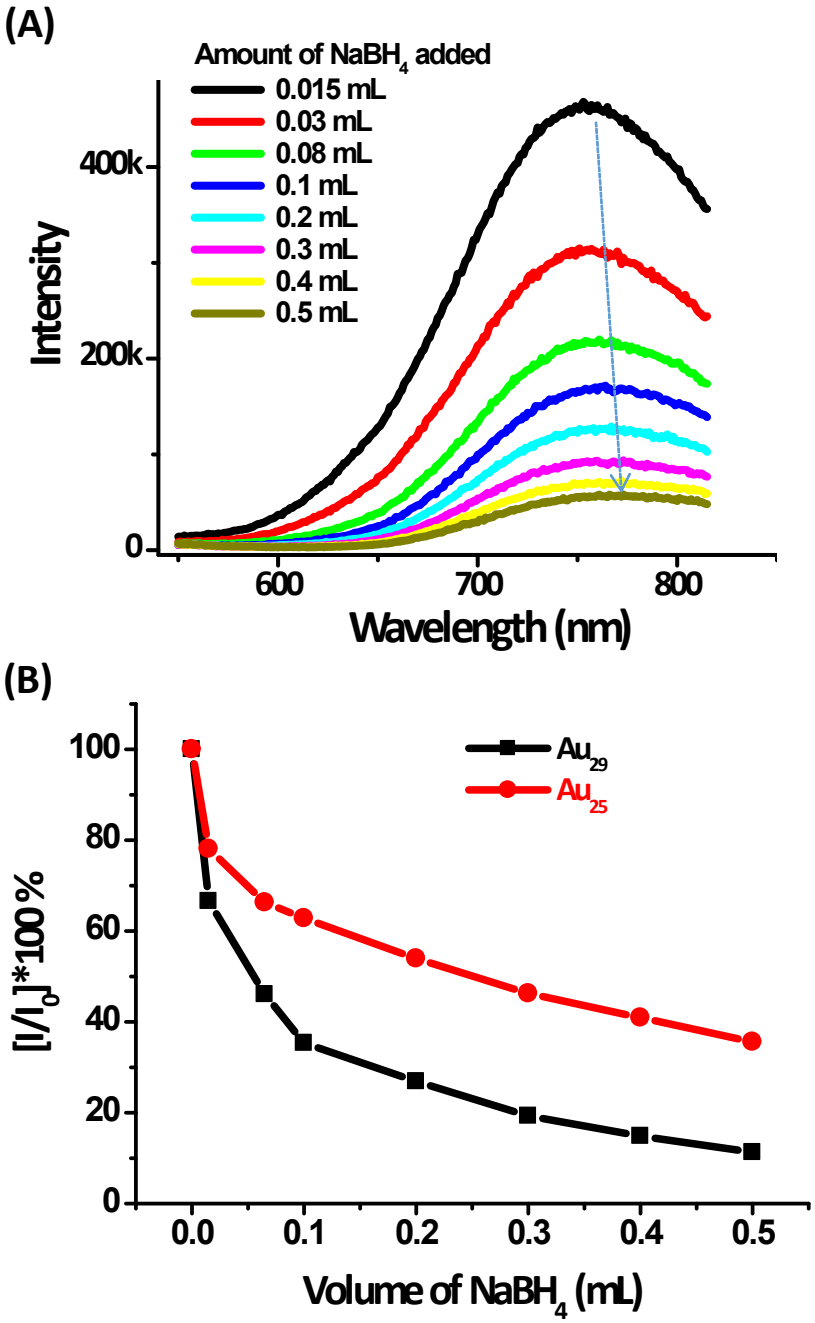

Figure S12. (A) Effect of addition of sodium borohydride to red luminescent Au_{29} cluster. With increasing amounts of $NaBH_4$ a emission intensities underwent a drastic quenching along with red shift possibly due to reduction of the surface thiolate shell on the cluster and thus shifting the luminescence to NIR regime. (B) Comparison of change in relative emission intensities of luminescent Au_{29} and parent $Au_{25}SBB_{18}$ cluster to equal amounts of $NaBH_4$.

Supporting information 13

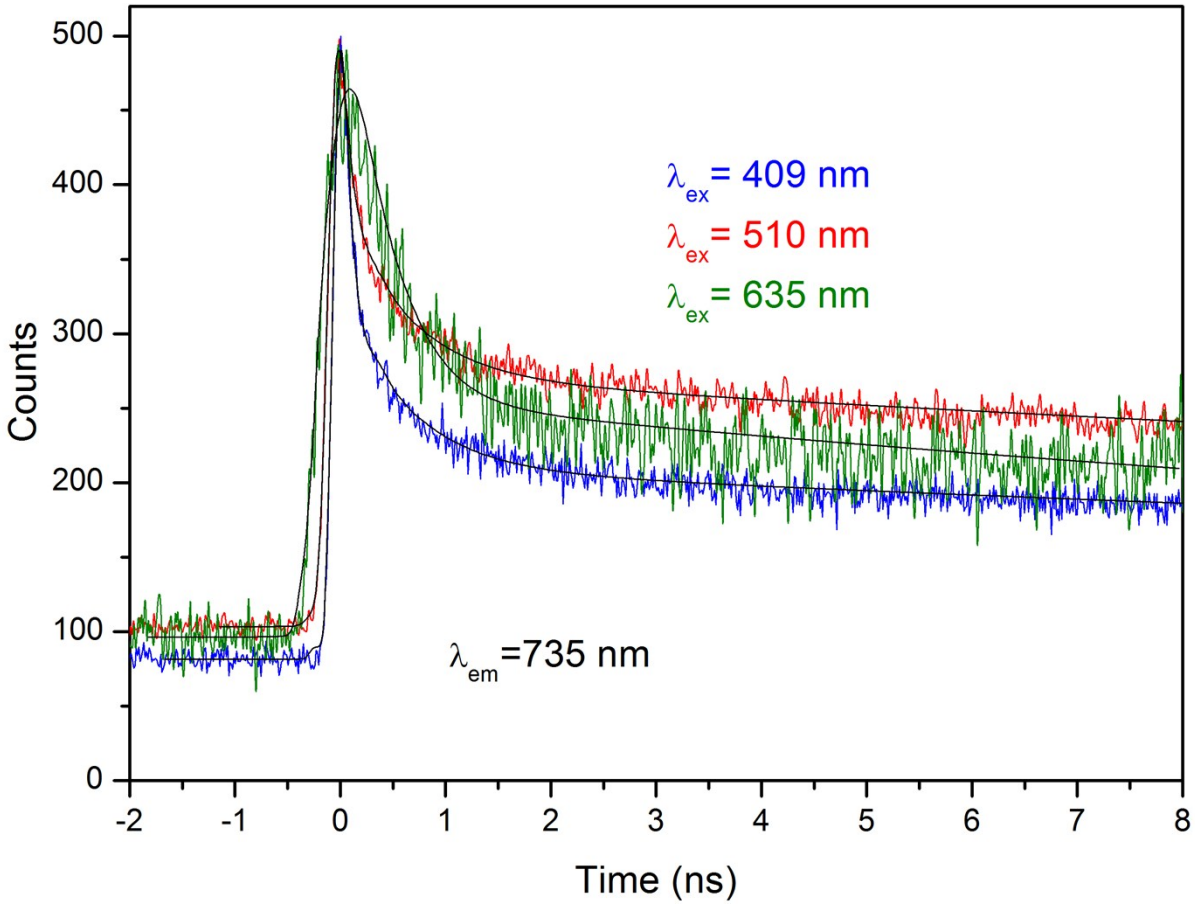

Figure S13. Life time decay of Au_{29} QCs (emission wavelength of 735 nm) upon excitation at different wavelengths.

Table S1. Picosecond time-resolved fluorescence transients of Au_{29} clusters in THF upon excitation in three different (409, 510 and 635 nm)

System in THF	τ_1(%) ns	τ_2(%) ns	τ_3(%) ns	τ_{avg} (ns)
Au_{29} (Ex 409 nm)	0.05(84)	0.79(8.5)	35(7.5)	2.77
Au_{29} (Ex 510 nm)	0.08(70)	0.814(18)	32(12)	4.02
Au_{29} (Ex 635 nm)	0.19(60)	1.09(26)	32(14)	4.87

Supporting information 14

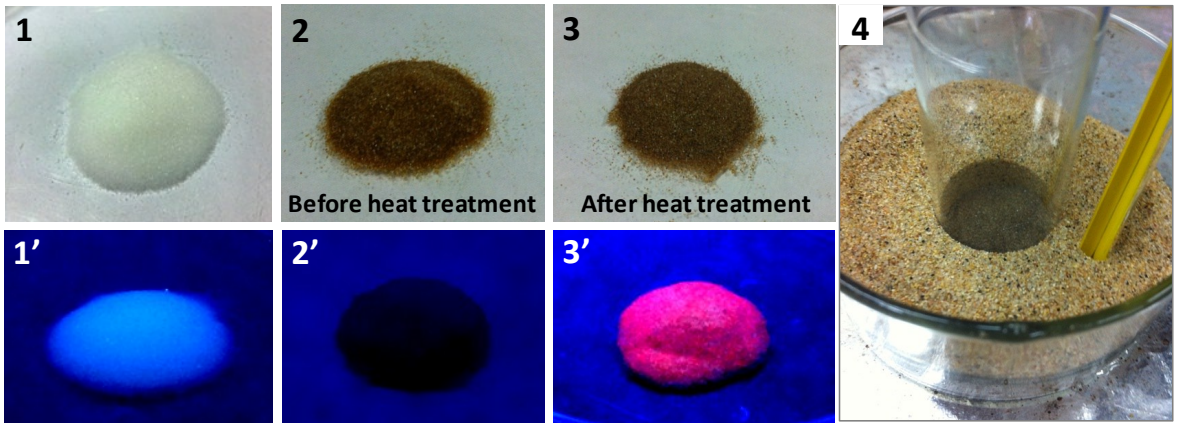

Figure S14. Photographs of of silica gel (1, 1'), $Au_{25}SBB_{18}$-loaded silica gel (2, 2') and $Au_{25}SBB_{18}$-loaded silica gel after 24 h heat treatment (3, 3') under visible light (1, 2 and 3) and under UV light (1', 2' and 3'). Experimental set-up is shown in (4). Though the $Au_{25}SBB_{18}$-loaded silica gel powder was initially non-luminescent (see 2, 2'), upon heating it became bright red luminescent (see 3 and 3') with little or no change in the visible color.